

METALLURGICAL STUDIES OF NITRONIC 40  
WITH REFERENCE TO ITS USE FOR CRYOGENIC  
WIND TUNNEL MODELS

David Wigley  
University of Southampton  
Southampton, England

A comprehensive study was carried out to investigate the characteristics of NITRONIC 40 in connection with its use in cryogenic wind tunnel models (ref. 1). In particular, the effects of carbide and sigma-phase precipitation resulting from heat treatment and the presence of delta ferrite were evaluated in relation to their effects on mechanical properties and the potential consequences of such degradation. (See figs. 1 through 20.)

Methods were examined for desensitizing the material and for possible removal of delta ferrite as a means of restoring the material to its advertised properties. It was found that heat treatment followed by cryogenic quenching is a technique capable of desensitizing NITRONIC 40. However, it was concluded that it is extremely difficult, if not impossible, to remove the delta ferrite from the existing stock of material. Furthermore, heat treatments for removing delta ferrite have to take place at temperatures that cause very large grain growth. The implications of using the degraded NITRONIC 40 material for cryogenic model testing were reviewed, and recommendations were submitted with regard to the acceptability of the material.

The experience gained from the study of NITRONIC 40 clearly identifies the need to implement a policy for purchasing top-quality materials for cryogenic wind tunnel model applications. The study also exemplifies the need for careful evaluation and analysis of processes used in the fabrication of metallic alloys for cryogenic use.

#### REFERENCE

1. Wigley, D. A.: The Metallurgical Structure and Mechanical Properties at Low Temperature of NITRONIC 40, With Particular Reference to Its Use in the Construction of Models for Cryogenic Wind Tunnels. NASA CR-165907, 1982.

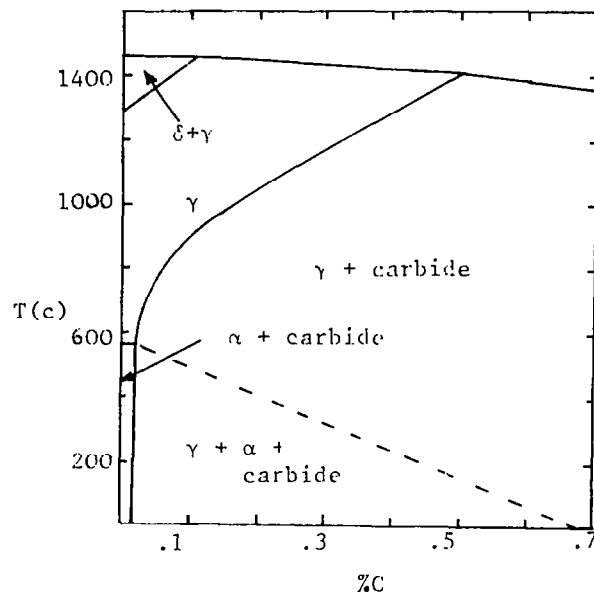


Figure 1.- Phase diagram for 18Cr-8Ni stainless steel. (From ref. 1.)

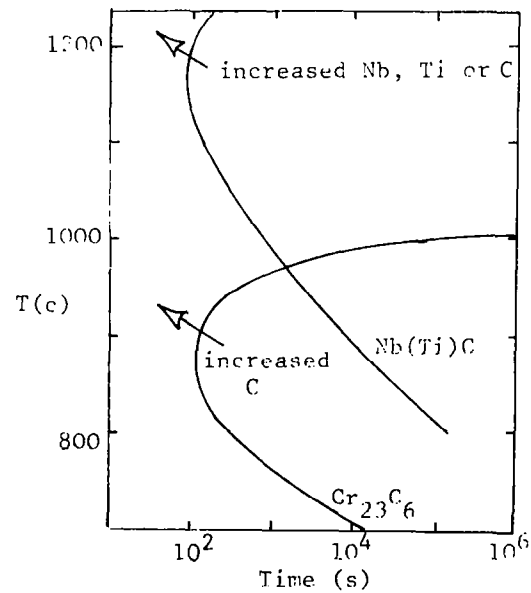


Figure 2.- T.T.T. (time-temperature transformation) curves for growth of  $\text{M}_{23}\text{C}_6$  and  $\text{Nb(Ti)C}$  in Cr-Ni stainless steel. (From ref. 1.)

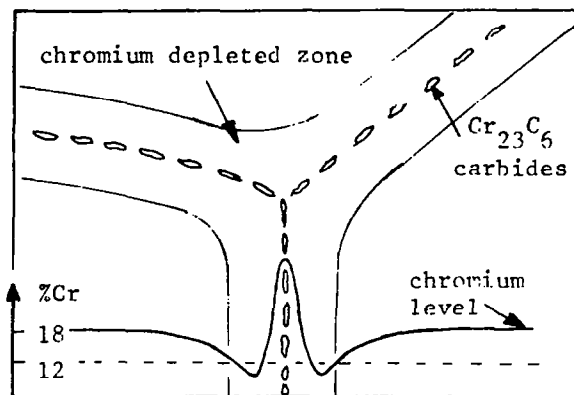


Figure 3.- Schematic representation of carbide precipitation and chromium depletion in 18/8 stainless steel. (From ref. 1.)

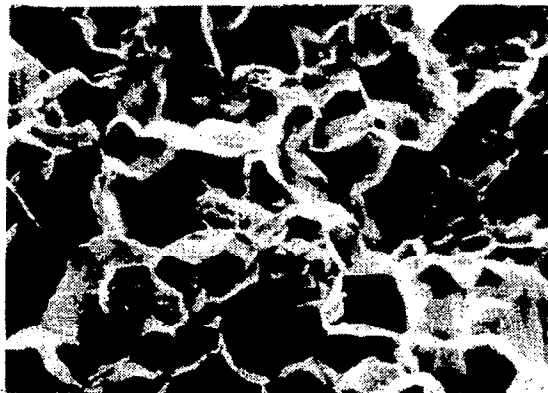
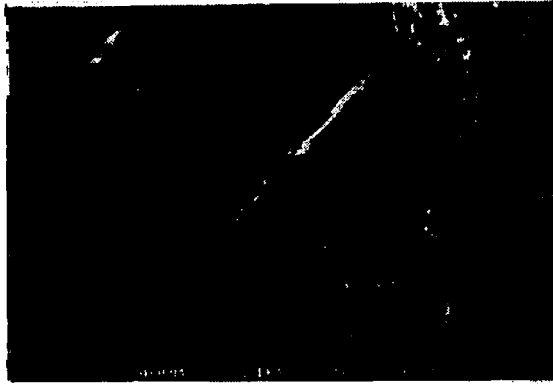
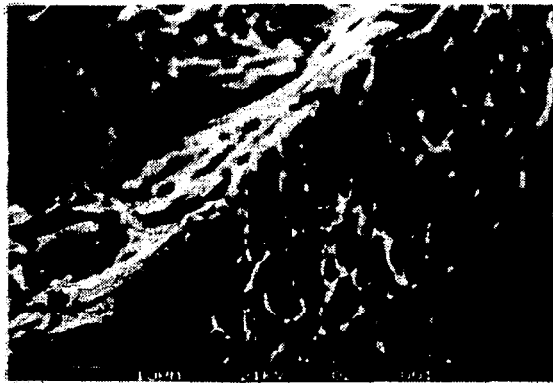


Figure 4.- Stereoscan view at x400 of intergranular fracture in 18/8 stainless steel. (From ref. 1.)

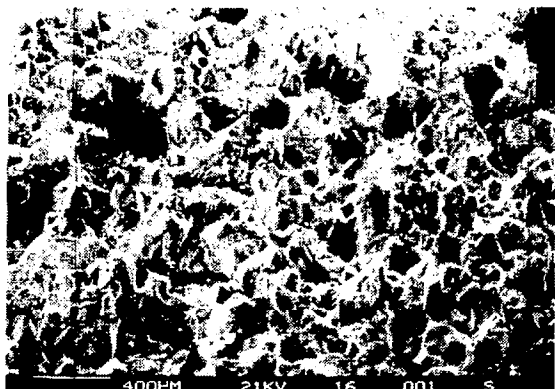


(a) Stereoscan, x400.

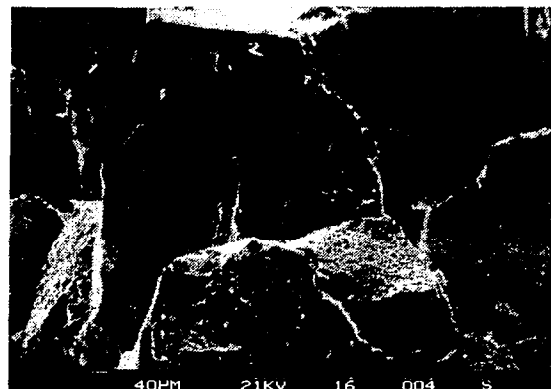


(b) Stereoscan, x1.6K.

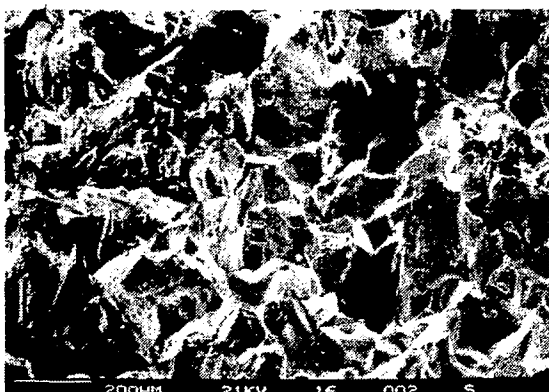
Figure 5.- Multiple nucleation of ductile dimples at grain boundary carbides during intergranular fracture of NITRONIC 40. (From ref. 1.)



(a) x30.



(d) x300.



(b) x60.



(e) x300.



(c) x120.

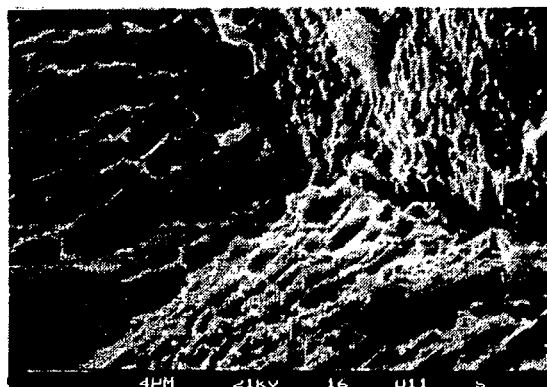


(f) x600.

Figure 6.- Stereoscan views of  $-320^{\circ}\text{F}$  Charpy fracture surface of highly sensitized NITRONIC 40. Specimen ST168. (From ref. 1.)

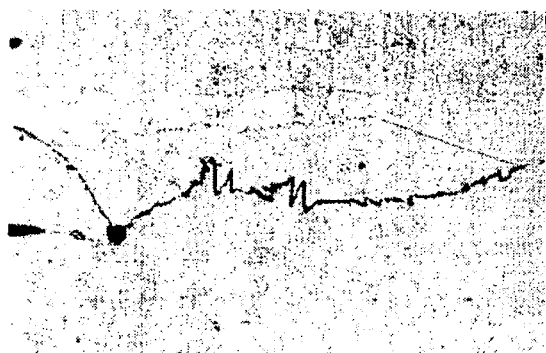


(g) x1.2K.

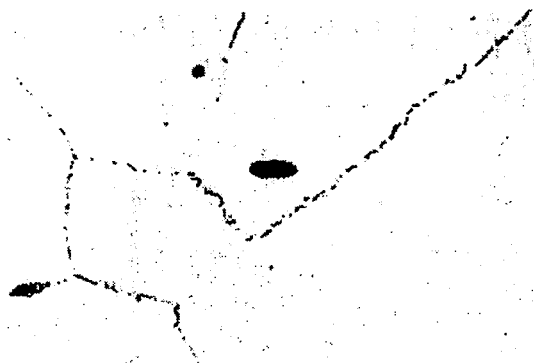


(h) x3K.

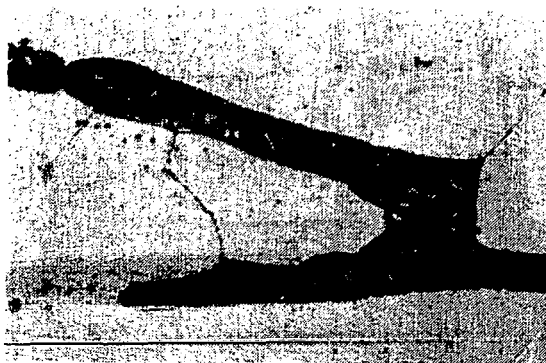
Figure 6.- Concluded.



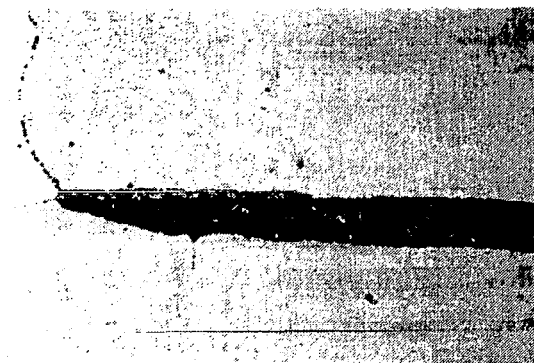
(a) ST5, x600.



(c) ST24, x600.

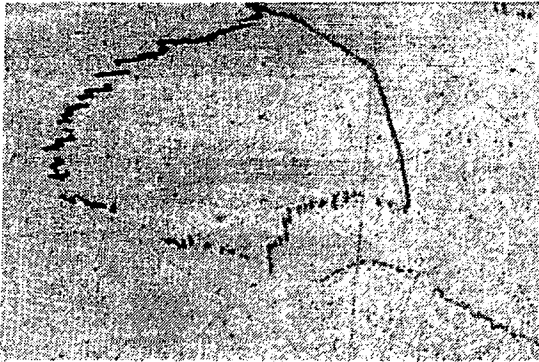


(b) ST5, x600.

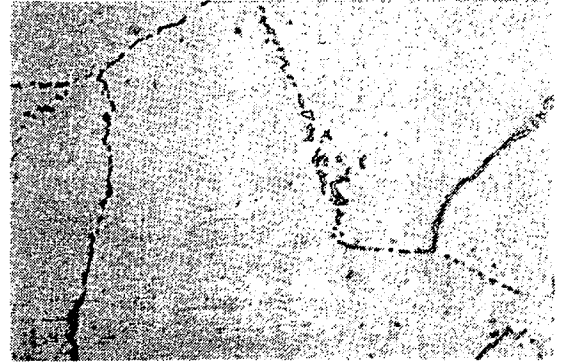


(d) ST24, x600.

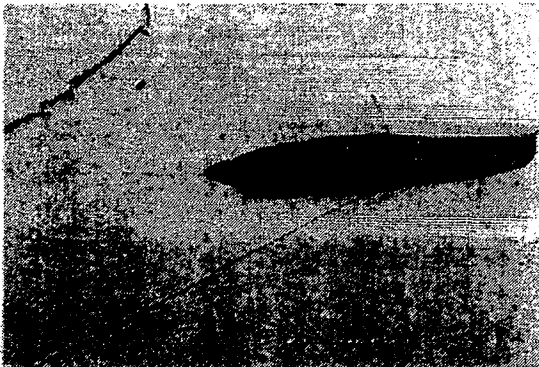
Figure 7.- Development of sigma-phase precipitates at grain boundaries and within delta ferrite during heat treatment at 1380°F (750°C) in sample S. (From ref. 1.)



(e) ST72, x600.



(g) ST168, x600.



(f) ST72, x600.



(h) ST168, x600.

Figure 7.- Concluded.



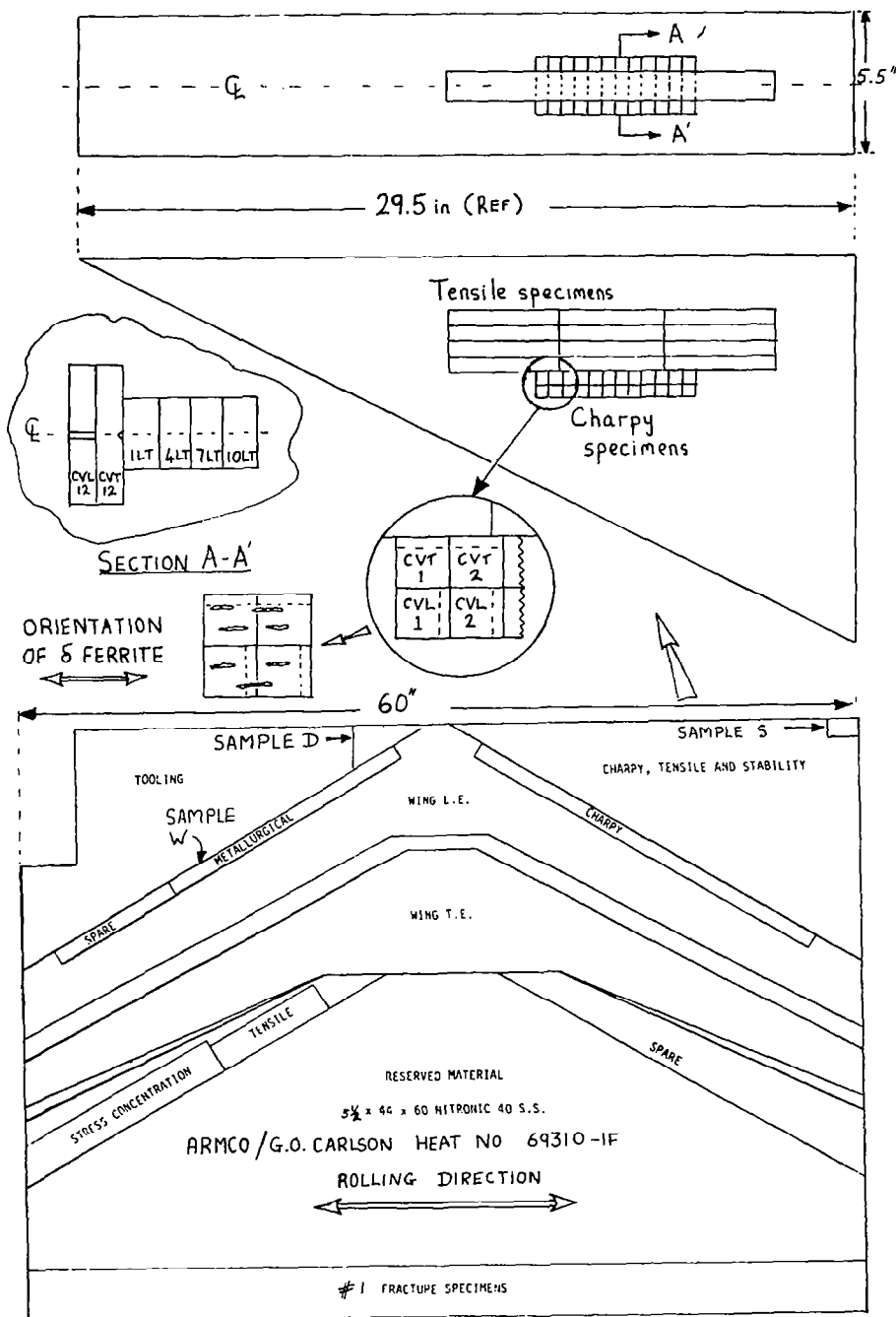


Figure 8.- Location of Charpies, tensiles, and samples D, S, and W.  
(From ref. 1.)

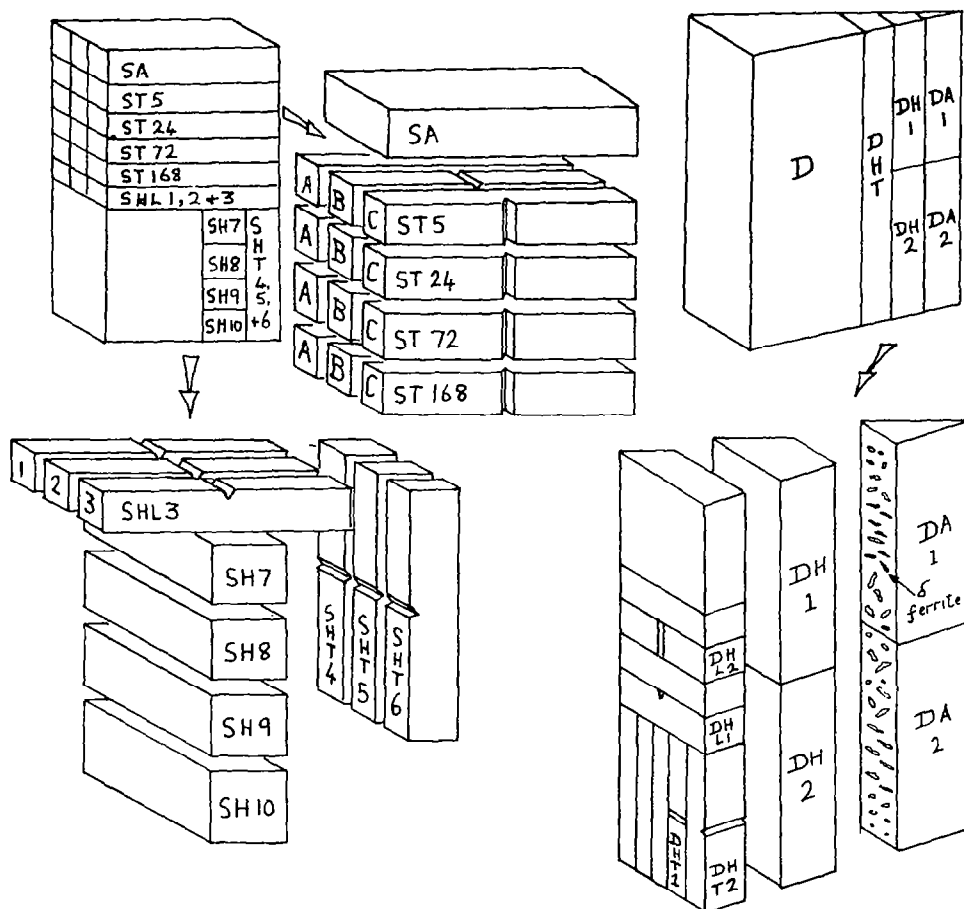


Figure 9.- Location of specimens in samples S and D from 5.5-in. plate.  
(From ref. 1.)

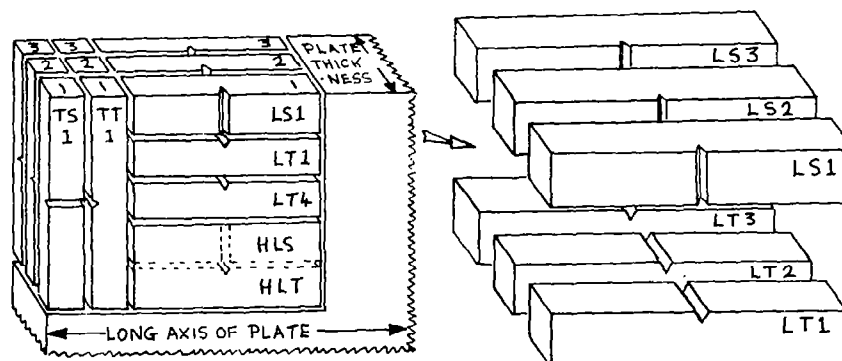


Figure 10.- Location of specimens in samples M and L  
from 1.25-in. plate. (From ref. 1.)

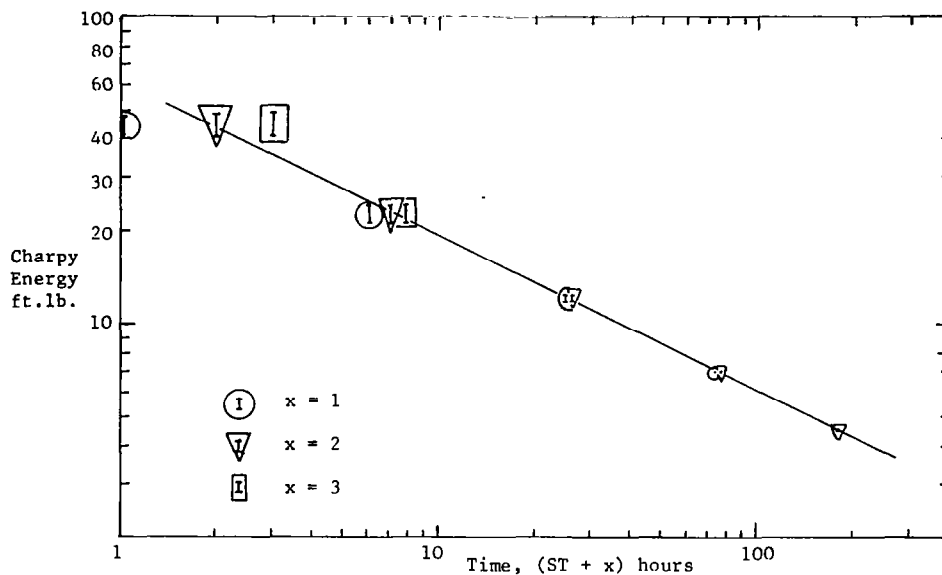


Figure 11.- Relationship between Charpy energy and sensitizing time in NITRONIC 40. (From ref. 1.)

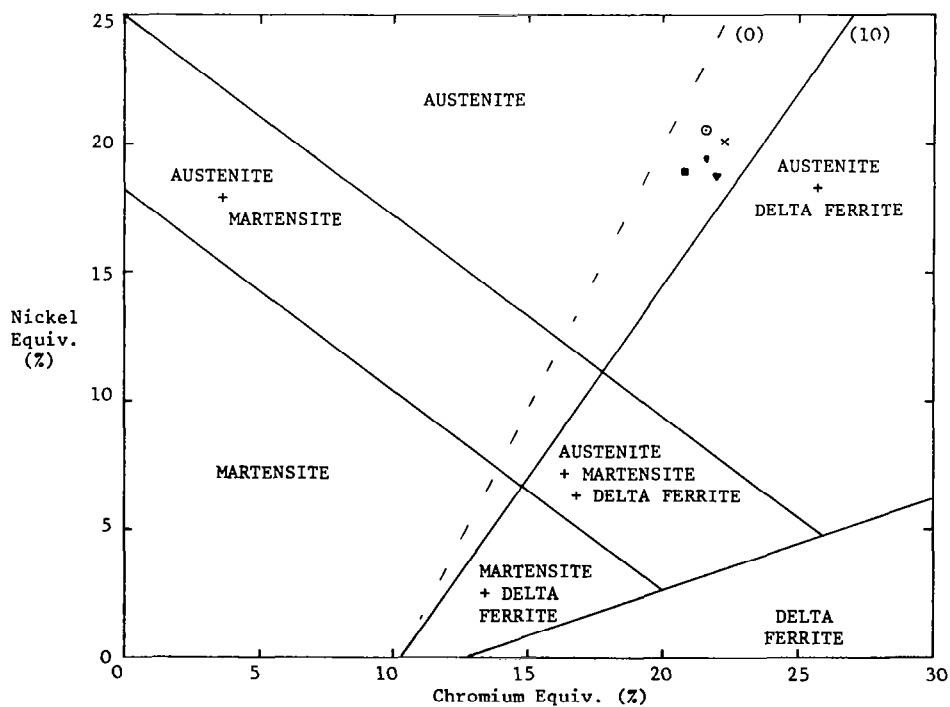
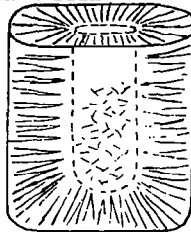


Figure 12.- Schaeffler diagram showing location of NITRONIC 40 samples. (From ref. 1.)

ARMCO/G.O. CARLSON  
HEAT No. 69310.

CAST INTO BILLET 52in x 21in

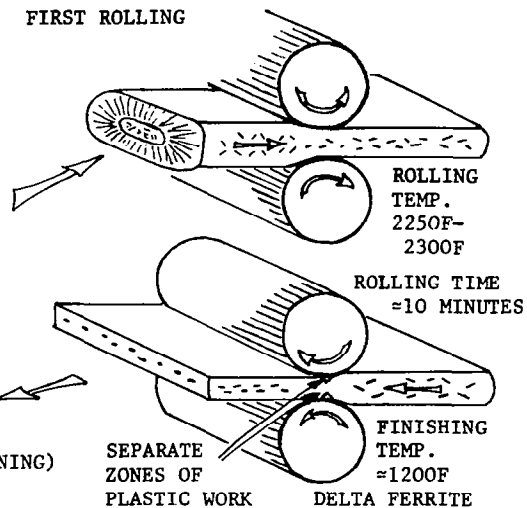
DENDRITIC GRAIN  
GROWTH FROM SURFACE  
CAUSES SEGREGATION  
OF ALLOYING  
ELEMENTS AND  
CONCENTRATION  
OF DELTA FERRITE  
WITH GRAIN BOUNDARY  
MORPHOLOGY AT  
CENTRE OF BILLET.



BILLET SIZE NOW  
12in thick x 50in wide x 50in long  
SURFACE DEFECTS GROUND OUT (CONDITIONING)

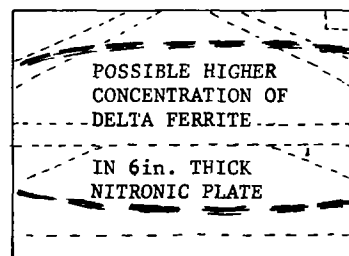
REHEATED TO 2275F FOR REROLLING DOWN  
TO 6in thick x 50in wide x 100in long.  
ENDS AND SIDES CUT OFF, ROLLED SURFACES  
GROUND TO GIVE SLAB 5.5in x 44in x 60in -  
DESIGNATED 69310-1F.

FIRST ROLLING



ZONES OF PLASTIC WORK DO NOT  
REACH CENTRE OF THICK PLATE:  
DELTA FERRITE LESS ORIENTED  
AT PLATE CENTRE

AS DELTA FERRITE ORIGINALLY  
IN MIDDLE OF BILLET, SIDES  
OF ROLLED SLAB PROBABLY  
CONTAIN LESS DELTA FERRITE  
THAN CENTRE, i.e. VARIATION  
OVER AREA OF PLATE



REMAINING MATERIAL FROM  
HEAT 69310 CROSS-ROLLED  
DOWN FROM 12in THICK.  
2in thick x 40in x 130in  
LANGLEY PLATE  
DESIGNATED 69310-1E.  
MCDONNELL DOUGLAS  
1.25in x 13in x 52in PLATE  
AND LOCKHEED 8 PLATES  
1.25in x 14in x 60in  
DESIGNATED 69310-1C.

CROSS ROLLING SPREADS  
DELTA FERRITE INTO DISCS  
WITH DIAMETER:THICKNESS  
RATIOS OF 10-20:1 AND  
SIMILAR DIAMETERS IN  
BOTH ROLLING DIRECTIONS.

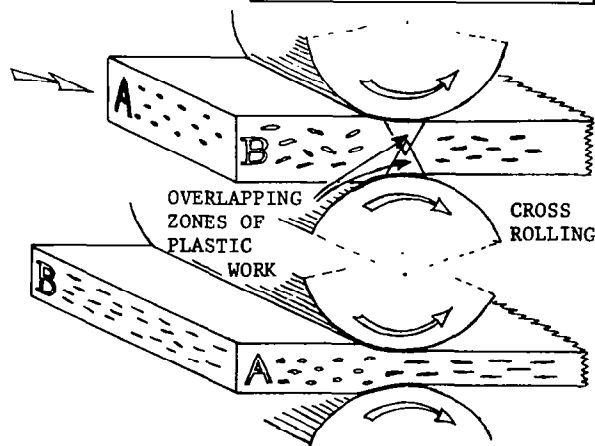
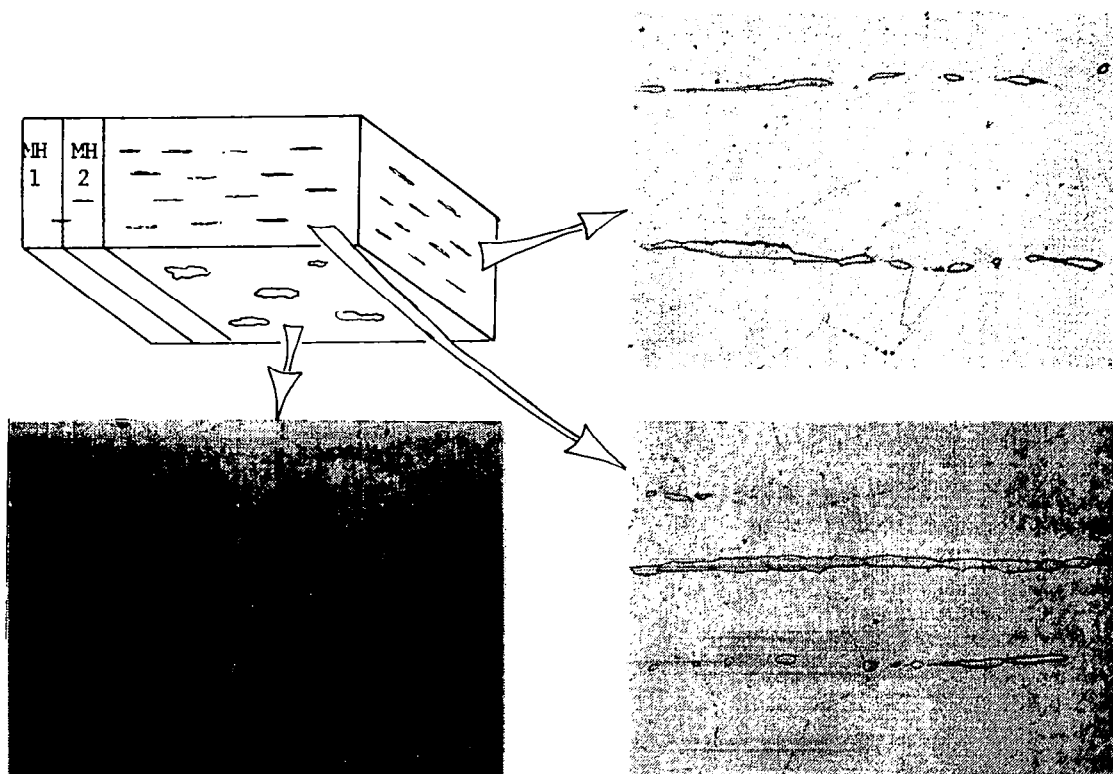
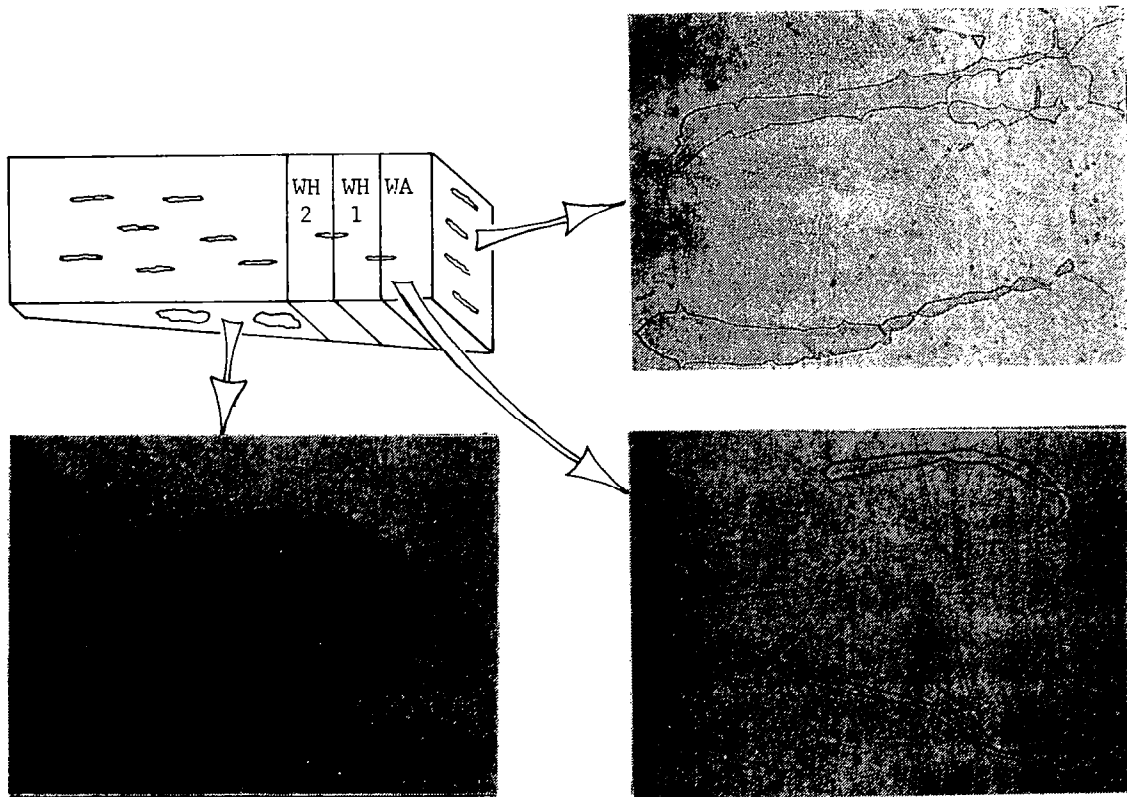


Figure 13.- Schematic representation of the effect of processing on the morphology of delta ferrite in NITRONIC 40. (From ref. 1.)



(a) McDonnell Douglas 1.25-in. plate (x300).

Figure 14.- Schematic representation of directionality in microstructure of two samples of rolled NITRONIC 40 plate. (From ref. 1.)

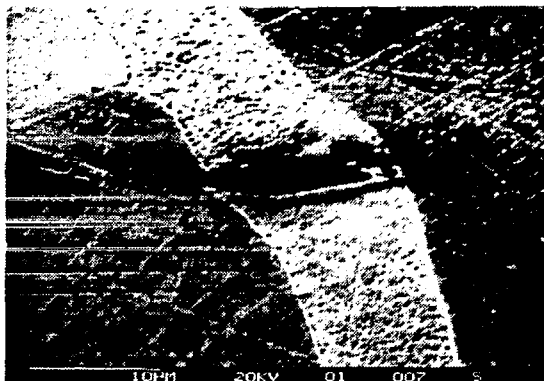


(b) Offcut from Langley 5.5-in. plate for Pathfinder I wing (x300).

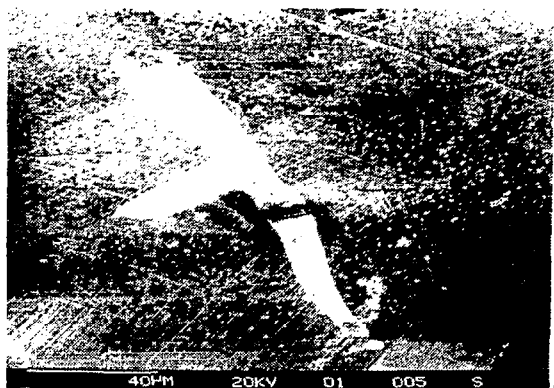
Figure 14.- Concluded.



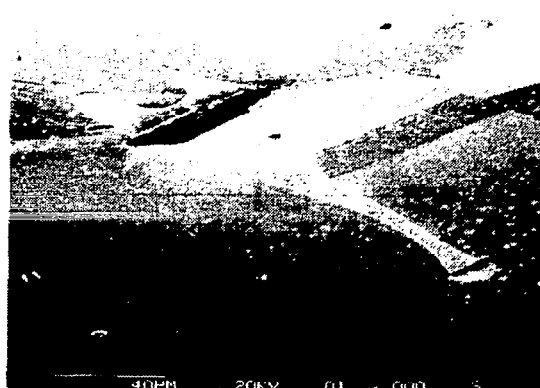
(a) x200.



(d) x2K.



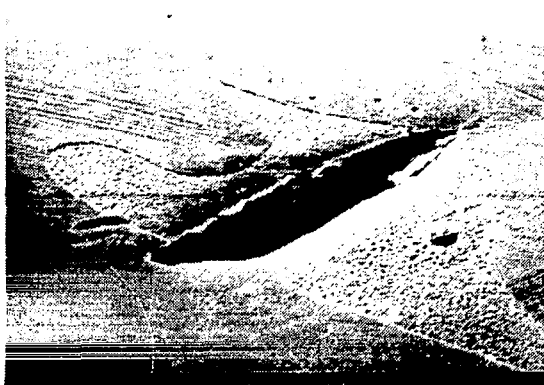
(b) x500.



(e) x500.



(c) x1K.



(f) x1K.

Figure 15.- Stereoscan views of cleavage cracks in delta ferrite on polished and etched surface adjacent to fracture. (From ref. 1.)

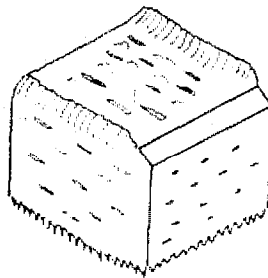
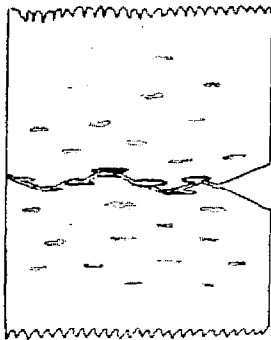


(g) x2K.

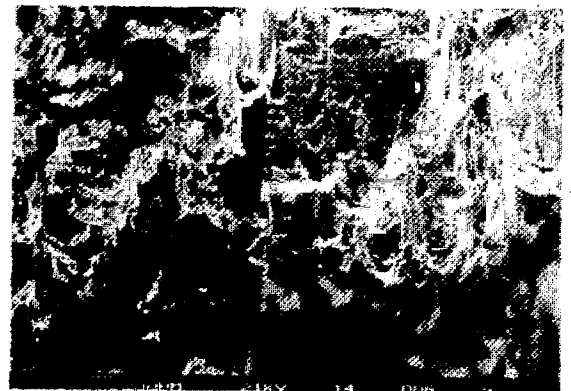


(h) x2K.

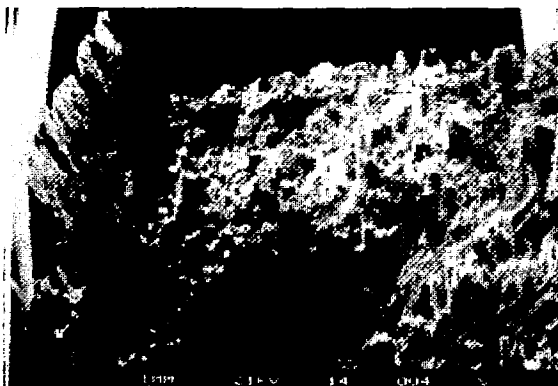
Figure 15.- Concluded.



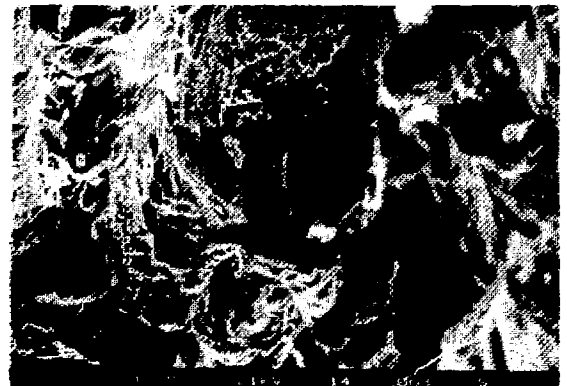
(a) Schematic view of SHT4.



(c) x63, 75° tilt.



(b) x13, 75° tilt.



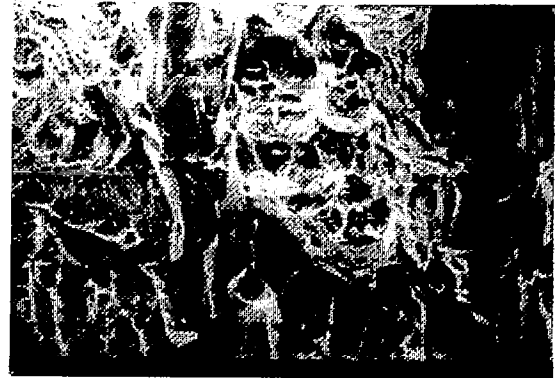
(d) x300, 75° tilt.

Figure 16.- Stereoscan fviews of 77 K Charpy fracture surface of desensitized NITRONIC 40 with delta ferrite oriented perpendicular to bar. (From ref. 1.)

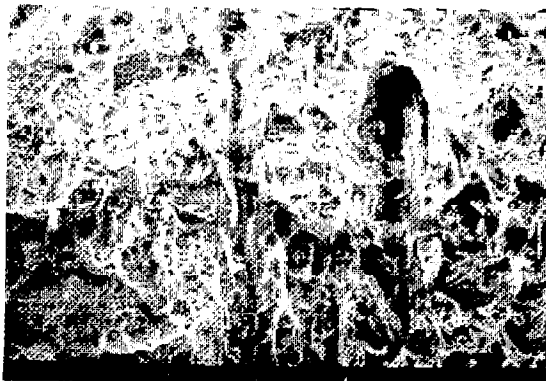




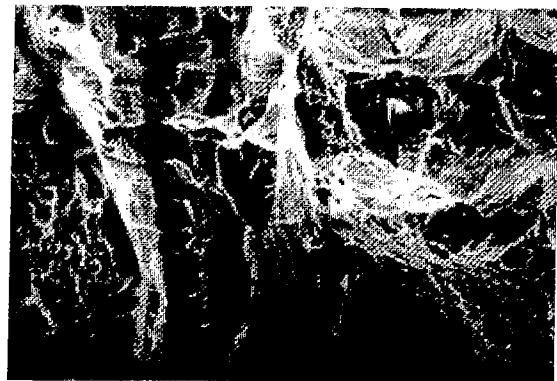
(e) x40, no tilt.



(g) x160.

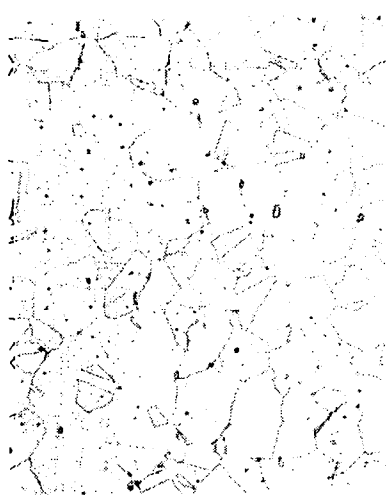


(f) x80.



(h) x400.

Figure 16.- Concluded.



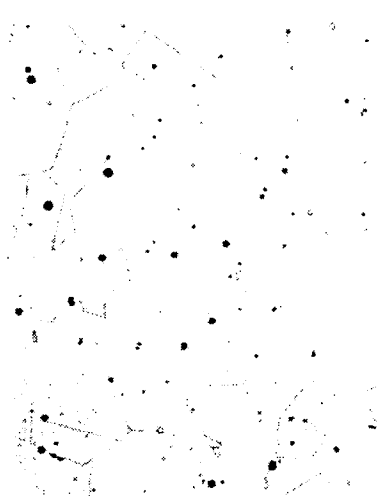
DA x50



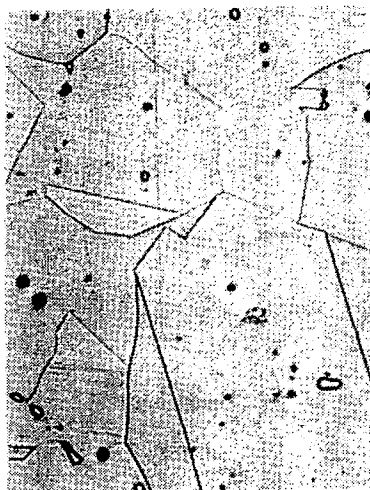
DA x100



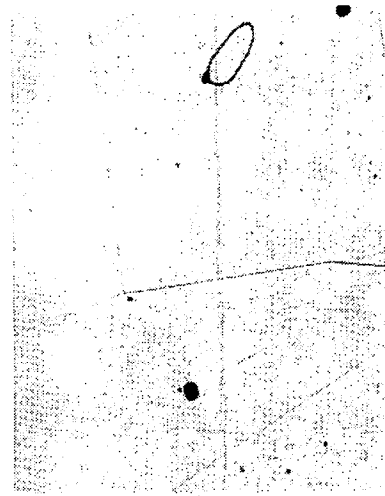
DA x300



DH1 x50



DH1 x100



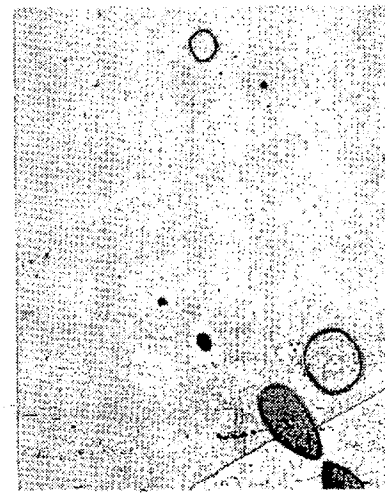
DH1 x300



DH2 x50



DH2 x100

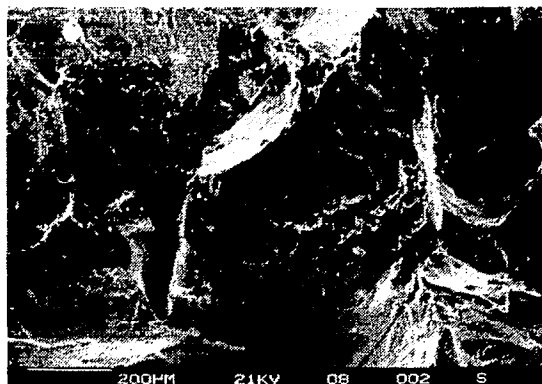


DH2 x300

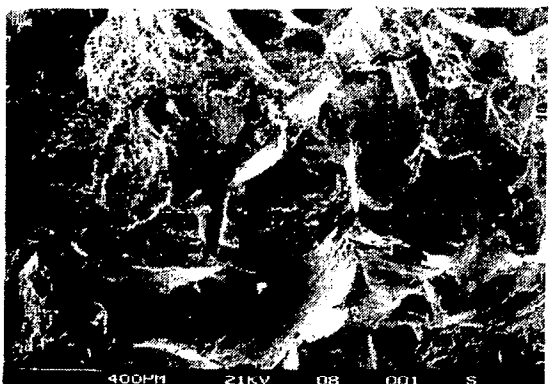
Figure 17.- Sample D. A = as received; H1 = 2200°F, 2 hr; H2 = 2200°F, 8 hr.  
(From ref. 1.)



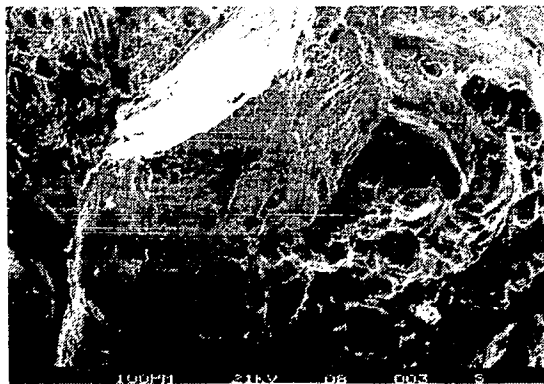
(a) x12.



(c) x60.

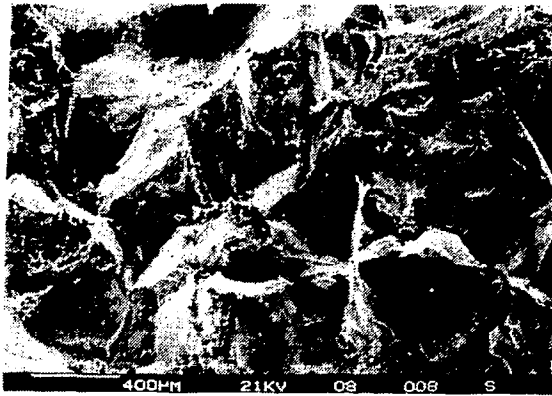


(b) x30.

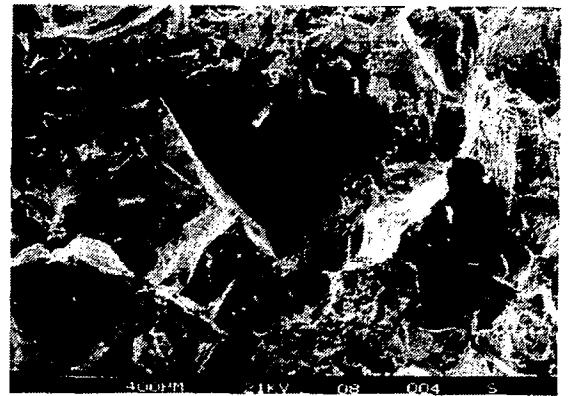


(d) x120.

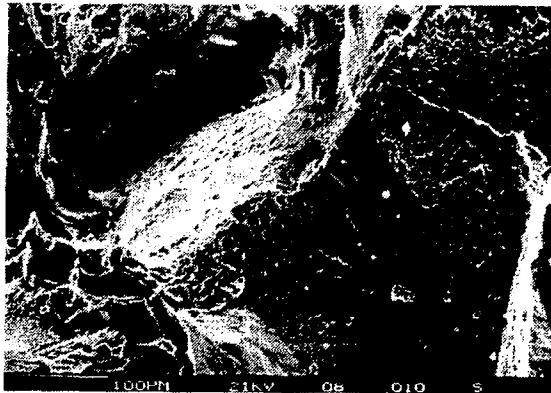
Figure 18.- Stereoscan views of  $-320^{\circ}\text{F}$  Charpy surface on NITRONIC 40 sample DH2 showing very large grains. (From ref. 1.)



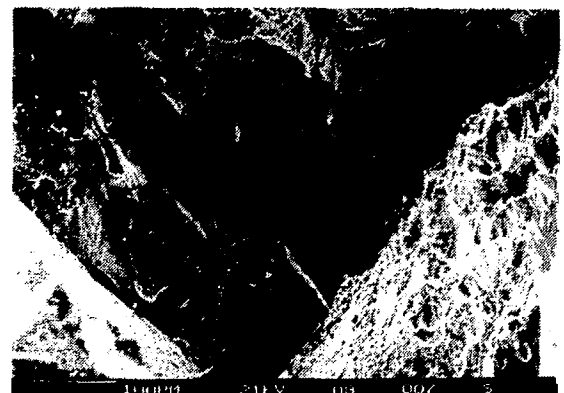
(e) x30.



(g) x30.



(f) x120.



(h) x120.

Figure 18.- Concluded.

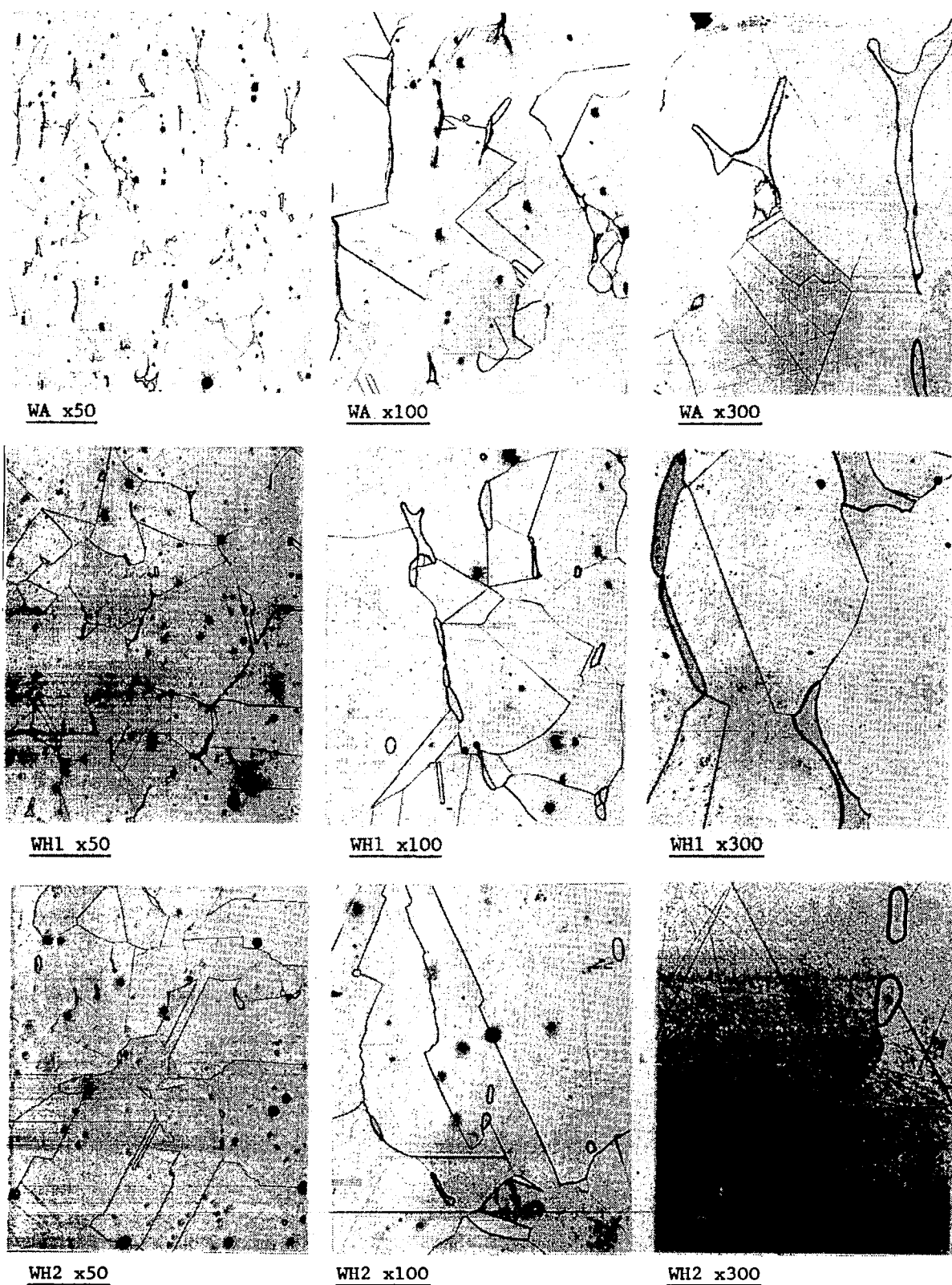
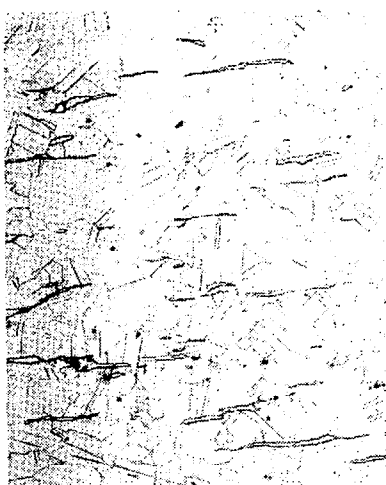


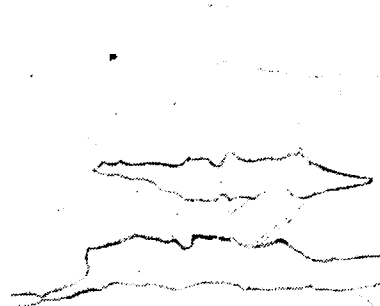
Figure 19.- Sample W. A = as received; H1 = 2200°F, 2 hr; H2 = 2200°F, 8 hr.  
(From ref. 1.)



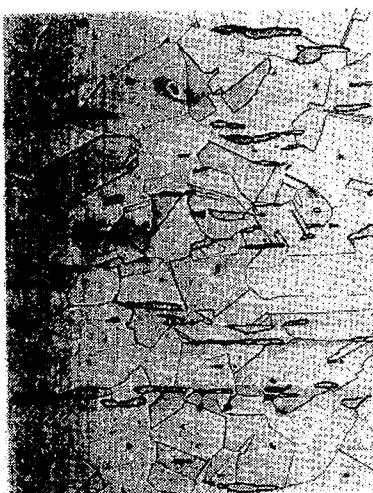
BA x50



BA x100



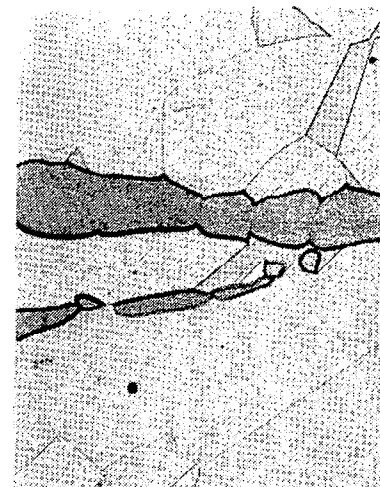
BA x300



BH1 x50



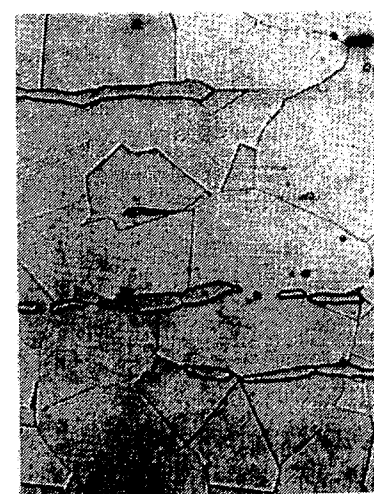
BH1 x100



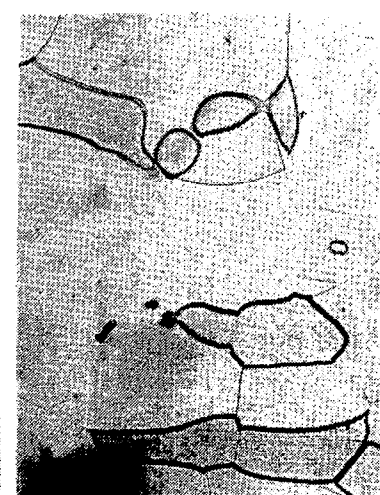
BH1 x300



BH2 x50



BH2 x100



BH2 x300

Figure 20.- Sample B. A = as received; H1 = 2200°F, 2 hr; H2 = 2200°F, 8 hr.  
(From ref. 1.)